# H5N1 Influenza Virus Pathogenesis in Genetically Diverse Mice Is Mediated at the Level of Viral Load

Adrianus C. M. Boon,[a] David Finkelstein,[b] Ming Zheng,[c] Guochun Liao,[c] John Allard,[c] Klaus Klumpp,[c] Robert Webster,[a] Gary Peltz,[c] and Richard J. Webby[a]

Department of Infectious Diseases[a] and Hartwell Center for Bioinformatics and Biotechnology,[b] St. Jude Children's Research Hospital, Memphis, Tennessee, USA, and Roche Pharmaceuticals, Palo Alto, California, USA[c]

**ABSTRACT** The genotype of the host is one of several factors involved in the pathogenesis of an infectious disease and may be a key parameter in the epidemiology of highly pathogenic H5N1 influenza virus infection in humans. Gene polymorphisms may affect the viral replication rate or alter the host's immune response to the virus. In humans, it is unclear which aspect dictates the severity of H5N1 virus disease. To identify the mechanism underlying differential responses to H5N1 virus infection in a genetically diverse population, we assessed the host responses and lung viral loads in 21 inbred mouse strains upon intranasal inoculation with A/Hong Kong/213/03 (H5N1). Resistant mouse strains survived large inocula while susceptible strains succumbed to infection with 1,000- to 10,000-fold-lower doses. Quantitative analysis of the viral load after inoculation with an intermediate dose found significant associations with lethality as early as 2 days postinoculation, earlier than any other disease indicator. The increased viral titers in the highly susceptible strains mediated a hyperinflamed environment, indicated by the distinct expression profiles and increased production of inflammatory mediators on day 3. Supporting the hypothesis that viral load rather than an inappropriate response to the virus was the key severity-determining factor, we performed quantitative real-time PCR measuring the cytokine/viral RNA ratio. No significant differences between susceptible and resistant mouse strains were detected, confirming that it is the host genetic component controlling viral load, and therefore replication dynamics, that is primarily responsible for a host's susceptibility to a given H5N1 virus.

**IMPORTANCE** Highly pathogenic H5N1 influenza virus has circulated in Southeast Asia since 2003 but has been confirmed in relatively few individuals. It has been postulated that host genetic polymorphisms increase the susceptibility to infection and severe disease. The mechanisms and host proteins affected during severe disease are unknown. Inbred mouse strains vary considerably in their ability to resist H5N1 virus and were used to identify the primary mechanism determining disease severity. After inoculation with H5N1, resistant mouse strains had reduced amounts of virus in their lungs, which subsequently resulted in lower production of proinflammatory mediators and less pathology. We therefore conclude that the host genetic component controlling disease severity is primarily influencing viral replication. This is an important concept, as it emphasizes the need to limit virus replication through antiviral therapies and it shows that the hyperinflammatory environment is simply a reflection of more viral genetic material inducing a response.

Genetic polymorphisms within the genome of the infected host play an important role in the response to and outcome of microbial infections. In humans, several polymorphisms that affect HIV, hepatitis C virus (HCV), and herpes simplex virus (HSV) pathogenesis (1–6) have been described. However, very few data are available on how host genetic differences influence the course of influenza A virus infection, and what is available is at best inconclusive. Studies on highly pathogenic H5N1 influenza virus in Asia support the notion of host genetic polymorphisms affecting susceptibility to H5N1 virus (7, 8), with a high proportion of infected contacts being genetically related to the index case within family clusters. Also, during the 2009 H1N1 virus pandemic, individuals of indigenous descent in the Americas, Austra-

lia, and the Pacific had higher hospitalization rates than did the overall population (9, 10). Although the increased incidence of risk factors such as diabetes and asthma may have contributed to this difference, gene polymorphisms likely played an important role in susceptibility to influenza virus.

Despite the evidence favoring a role for host genetic polymorphisms in susceptibility to influenza virus infection, no human polymorphisms have been discovered. More importantly, we have yet to understand the mechanistic basis for the difference in pathogenesis: does the genetic change in susceptible hosts allow for increased replication dynamics of the virus or an altered immune environment, or does it completely change the hosts' response to the pathogen independently of viral burden? Existing

literature reporting large differences in the host responses after infection with low- or highly pathogenic viruses (11–17) would suggest that individuals with severe disease have an aberrant immune response to the virus. Alternatively, the genetic differences between the hosts allow for an increased virus replication rate, resulting in the induction of a more vigorous immune response. In humans, H5N1 virus pathogenesis is characterized by high viral load and increased production of proinflammatory cytokines culminating in severe disease and often death (i.e., 60% mortality rate in humans) (12, 15). Due to the correlative nature of the 2 parameters, it is unclear how they are linked and how each affects survival after infection. The importance of replication dynamics was recently highlighted in a paper by Hatta et al. demonstrating that the more virulent H5N1 virus also had the highest replication rate of the viruses studied (18).

To increase our understanding of H5N1 virus pathogenesis and to study the effects of host genetic variation, we initiated a large systematic effort to define the underlying mechanism involved in susceptibility or resistance to influenza virus infection. This knowledge is crucial for the identification of genes or gene networks associated with differences in pathogenesis. In summary, H5N1 virus pathogenesis in genetically diverse hosts is largely determined by the host factors controlling viral load in the lungs. Increased viral loads initiate the production of excessive amounts of proinflammatory cytokines, causing tissue damage and ultimately mortality of the susceptible host.

## RESULTS

**H5N1 virus pathogenic phenotypes among inbred mouse strains.** We experimentally inoculated 21 mouse strains with the highly pathogenic H5N1 influenza A virus A/Hong Kong/213/03 (HK213) and monitored the animals for 30 days thereafter for signs of morbidity and mortality. The 50% mouse lethal dose ($MLD_{50}$) values varied from 40 50% egg infective doses ($EID_{50}$) for the influenza virus-susceptible strain $DBA/2_S$ (susceptibility indicated by "S") to more than $10^6$ $EID_{50}$ for the influenza virus-resistant strains $BALB/c_R$ and $BALB/cBy_R$ (resistance indicated by "R") (Fig. 1).

Several strains were resistant to the high-dose challenge and had $MLD_{50}$ values between $10^5$ and $10^6$ $EID_{50}$. Others were considered either susceptible ($MLD_{50} < 10^4$ $EID_{50}$) or highly susceptible ($MLD_{50} < 10^3$ $EID_{50}$). The diversity in pathogenic potential of a single highly pathogenic H5N1 virus prompted us to define a dose of virus that was lethal to the susceptible mouse strains but induced only mild morbidity without mortality in the resistant strains. Thus, we set the dose of $10^4$ $EID_{50}$ as the cutoff for H5N1 virus resistance/susceptibility and subsequently used it in all host response experiments.

**Transfer of hematopoietic cells from resistant strains does not rescue the pathogenic phenotype of susceptible strains.** An appropriate immune response mediated by hematopoietic cells is essential for clearance of influenza viruses and subsequent survival of the infected host. To test whether susceptible mouse strains have an inferior immune response due to one or more genetic polymorphisms, we generated chimeric $DBA/2_S$ mice whose bone marrow (BM) was replaced with that of $C57BL/6_R$ ($DBA/2_{C57}$), $BALB/c_R$ ($DBA/2_{BALB}$), or $DBA/2_S$ ($DBA/2_{DBA/2}$) as a control. Twelve weeks post-BM transfer, successful engraftment was determined using strain-specific cell surface markers. The chimeric mice were subsequently infected with 1 of 2 doses of HK213 virus.
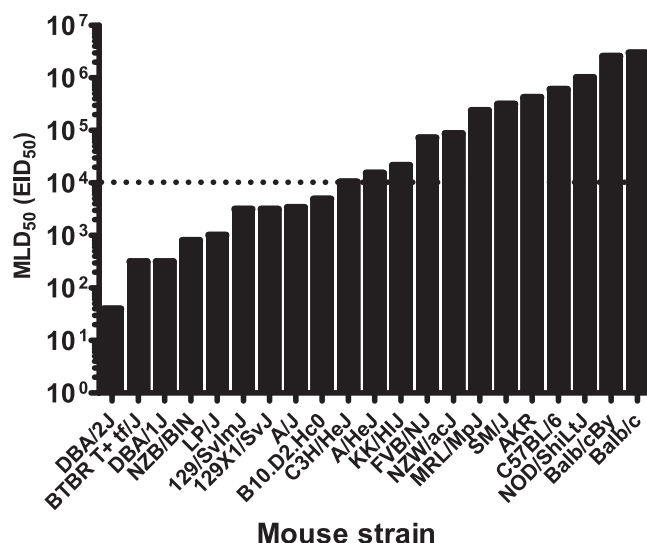


**FIG 1** Pathogenic profile of 21 inbred mouse strains inoculated with highly pathogenic H5N1 influenza A virus. The 50% mouse lethal dose ($MLD_{50}$) of A/Hong Kong/213/03 virus is shown. A dose of $10^4$ $EID_{50}$ (dotted line) was set to distinguish influenza virus-resistant from influenza virus-susceptible mouse strains and used throughout the work to assess biological parameters associated with severity of disease and mortality.

At a dose of $10^4$ $EID_{50}$, the $DBA/2_{C57}$ and $DBA/2_{BALB}$ mice succumbed to infection approximately 7 to 8 days postinoculation (dpi). This finding was similar to that seen in age-matched DBA/2 control mice and $DBA/2_{DBA/2}$ mice (Fig. 2A). Intranasal inoculation with a 10-fold-lower dose ($10^3$ $EID_{50}$) produced similar results: $DBA/2_{BALB}$ mice died around the same time (postinoculation day 8) as did the $DBA/2_{DBA/2}$ control mice. $DBA/2_{C57}$ mice survived a few days longer; however, all of the mice had died by day 12 postinoculation (Fig. 2B). Thus, the immune response of hematopoietic origin from resistant mouse strains was unable to rescue the phenotype of a susceptible strain, consistent with the hypothesis that the genetic polymorphism(s) affecting H5N1 virus pathogenesis in susceptible mouse strains promotes viral replication in the epithelial cells of the respiratory tract.

**RNA expression profile early after H5N1 virus infection differentiates susceptible from resistant mouse strains.** To identify differences in the molecular responses to HK213 virus infection in the susceptible and resistant mouse strains, we performed large-scale expression analysis of lung tissue before and at various time points after inoculation in 3 susceptible strains ($DBA/2_S$, $129/SvIm_S$, and $A/J_S$) and 3 resistant strains ($SM_R$, $C57BL/6_R$, and $BALB/c_R$). Probes (26,000) that were detected in one or more strains at any time point after infection were included in subsequent analyses. Prior to detailed gene and pathway expression analysis, we performed an unsupervised principal component analysis (PCA) to identify similarities or differences in overall gene expression between strains of mice before inoculation and 1, 3 and 7 days postinoculation (dpi). If all biological replicates of a particular condition (mouse strain) form a cluster and are located elsewhere on the plot compared to the rest of the data, that particular mouse strain is considered to have a distinct expression profile. Our goal was to identify similarities and differences among the strains and correlate those with our disease phenotype. Prior to infection or shortly thereafter (day 1 postinfection), no
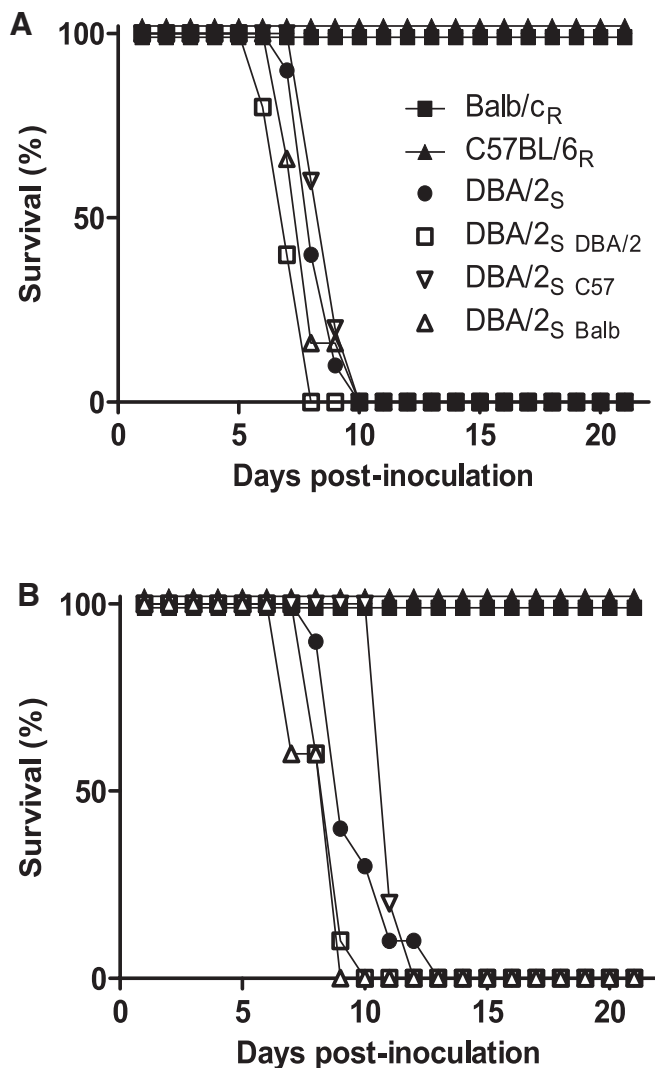
**FIG 2** The hematopoietic component does not confer resistance in susceptible strains. Chimeric $DBA/2_S$ mice containing bone marrow from resistant ($C57BL/6_R$ or $BALB/c_R$) or susceptible ($DBA/2_S$) mice were inoculated with $10^4$ $EID_{50}$ (A) or $10^3$ $EID_{50}$ (B) of A/Hong Kong/213/03 virus and monitored for morbidity and mortality for 21 days.

clustering was observed, and individual data were scattered throughout the plot (Fig. 3). At day 3 postinfection, the expression profiles of the mice clustered into 3 groups. Group 1 (red circle) contained only highly susceptible strains ($DBA/2_S$ and 129/$SvIm_S$). Group 2 (green circle) was composed of resistant strains ($C57BL/6_R$ and $BALB/c_R$) only. Group 3 (blue circle) was composed of a susceptible strain and a resistant strain ($A/J_S$ and $SM_R$, respectively) and was situated between groups 1 and 2 on the second component. By day 7, the clustering of susceptible (group 1) and resistant (group 2) strains remained intact. More importantly, the susceptible strain in group 3, $A/J_S$, had joined group 1, and the resistant strain ($SM_R$) was found in close proximity to the other resistant strains of group 2. These plots clearly indicate that a gene expression signature is associated with death or survival in these mice but also that these signatures are not necessarily fixed until later in the infectious process.

**Pathway analysis of the response to H5N1 virus infection in inbred mouse strains.** To identify qualitative and quantitative differences in the host responses associated with survival, we probed the transcriptomes of susceptible and resistant mouse strains before and after inoculation with H5N1 virus. Because our phenotype occurred after H5N1 virus infection, we focused on genes whose expression increased or decreased ≥2-fold compared to that in uninfected controls in at least two of the three susceptible or resistant mouse strains; this approach yielded a comprehensive set of 2,038 genes.

At day 1 postinoculation, 76 genes were differentially expressed, of which the majority (64) were shared by the susceptible and resistant strains (see Fig. S1A in the supplemental material). By day 3, the number of differentially expressed genes increased dramatically to 829, and 569 (68.6%) of those were shared by the two groups. Surprisingly, only 28 (3.4%) genes were uniquely up- or downregulated in the resistant strains and 232 (70.5%) were found only in the susceptible strains. These included several genes that encode cytokines associated with increased inflammation, e.g., *Il28b*, *Ifna4*, *Ifna5*, and *Tnfrsf1b*. Similar results were found at day 7, with 582 of 1,084 (53.7%) genes differentially expressed in the susceptible strains only. Overall, these data suggest that the resistant mouse strains do not express a unique set of genes or a pathway(s) controlling replication or disease. Rather, the difference in expression profiles identified by PCA (Fig. 3) was caused by altered or increased gene expression in the susceptible mouse strains.

Next, we performed pathway analysis of the up- or downregulated genes within each mouse strain. At day 1 postinoculation, gene sets in 5 of 6 strains were enriched for the glutathione pathway ($SM_R$ was the exception). By day 3, the identified pathways were similar among all 6 strains (see Fig. S1B in the supplemental material), with significant *P* values for all the well-known pathways, including the cytokine-cytokine receptor interaction pathway, Toll-like receptor pathway, NOD-like receptor pathway, and chemokine signaling pathway. The increased expression of many of these pathway-associated genes in all strains suggested that the difference in resistance to H5N1 virus pathology is not due to a defect in innate or antiviral immune signaling in the susceptible strains. On the contrary, our analysis of the total number of genes identified within a particular pathway (Fig. S1C) showed many more upregulated genes in the $DBA/2_S$ and 129/$SvIm_S$ strains than in other strains. At day 7 postinfection, we found an enriched gene expression profile in the resistant mouse strains that is associated with systemic lupus erythematosus, cell adhesion molecules, the antigen processing and presentation pathway, and the graft-versus-host disease pathway. This profile is indicative of adequate virus-specific T- and B-cell responses in these mice. In contrast, the 3 susceptible strains continued to have many cytokine genes upregulated, as evidenced by the low *P* value for the cytokine-cytokine receptor interaction pathway (Fig. S1B and S1C; Table S1).

Finally, we performed statistical analysis on the array data to identify genes whose expression values correlated with the PCA clustering observed on days 3 and 7 postinoculation (see Table S2 in the supplemental material). The majority of the 85 identified genes belonged to proinflammatory pathways, including cytokine-cytokine receptor pathways, the Jak-Stat pathway, and innate sensing pathways like the Toll-like receptor pathway. To summarize, the difference between resistant and susceptible
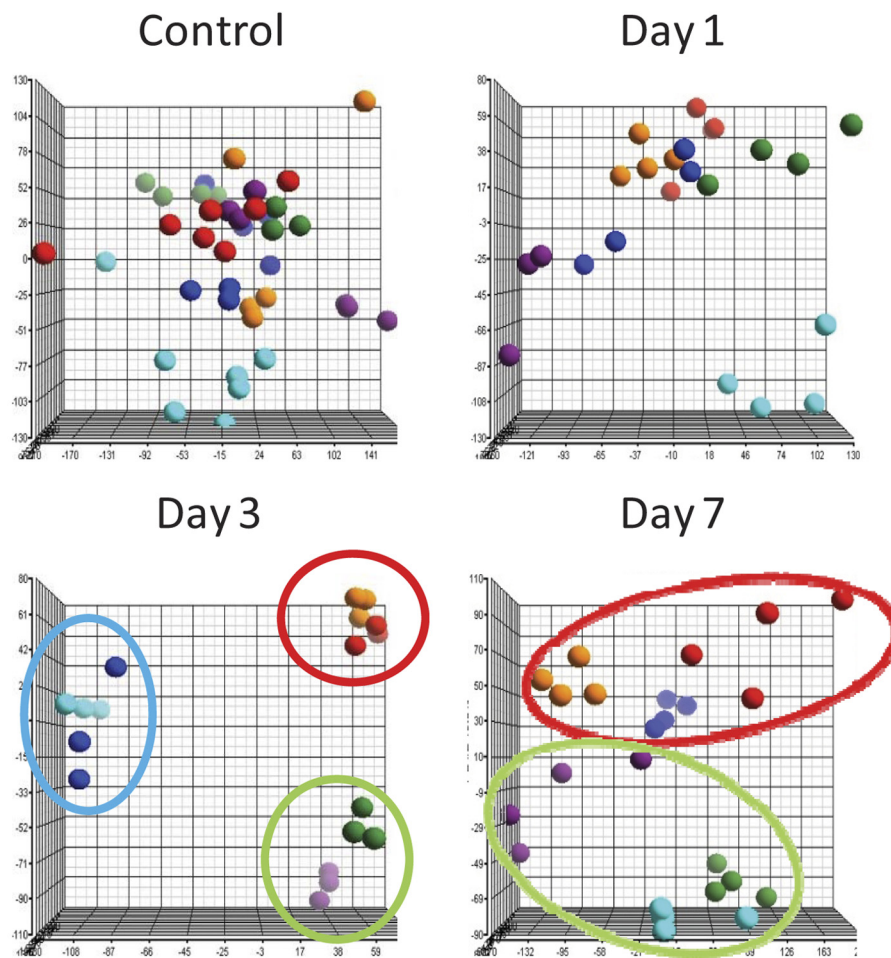
FIG 3 Principal component analysis identifies the gene expression profile associated with severity of H5N1 virus disease. Principal component analysis using ~26,000 probes in lung tissue RNA of DBA/$2_S$, 129/SvIm$_S$, A/J$_S$, SM$_R$, C57BL/6$_R$, and BALB/c$_R$ mice prior to infection (control) and on days 1, 3, and 7 after inoculation with $10^4$ EID$_{50}$ of A/Hong Kong/213/03. Each dot represents the RNA expression profile of a single mouse. Colored circles indicate the three clusters of highly susceptible (red), intermediate susceptible (blue), and resistant (green) mouse strains. The x, y, and z axes correspond to principal components 1, 2, and 3, respectively.

strains is predominantly quantitative, with the excessive production of proinflammatory cytokines in the susceptible strains most likely affecting downstream induction of robust adaptive immune responses. The overrepresentation of proinflammatory genes in the susceptible strains is indicative of ongoing viral replication and suggests higher replication rates and higher viral loads in these strains.

**Increased production of inflammatory mediators in susceptible mouse strains.** Many of the genes associated with severe disease that were identified by expression analysis are considered proinflammatory. Although inflammation is important for the induction of an innate and adaptive immune response, too much inflammation can be pathological and exacerbate disease. To validate the expression data and demonstrate increased production of proinflammatory mediators in the susceptible strains, we measured the production of CCL2, alpha interferon (IFN-$\alpha$), IFN-$\beta$, tumor necrosis factor alpha (TNF-$\alpha$), CXCL2, and CSF3 after inoculation with $10^4$ EID$_{50}$ in 3 susceptible mouse strains (DBA/$2_S$, 129/SvIm$_S$, and A/J$_S$) and 3 resistant strains (SM$_R$, C57BL/6$_R$, and BALB/c$_R$). At day 3 postinfection, lung homogenates of sus-

ceptible strains contained significantly higher concentrations of proinflammatory cytokines than did those of most of the resistant strains (Fig. 4); however, intriguing patterns emerged. The concentration of CSF3 was significantly higher in all susceptible strains and in the SM$_R$ strain, which, based on expression analysis, clustered with the susceptible A/J$_S$ strain. A similar pattern was found for IFN-$\alpha$ and IFN-$\beta$. In contrast, the production levels of CCL2 and CXCL2 were significantly higher in the DBA/$2_S$ and 129/SvIm$_S$ strains than in the other 4 strains. Finally, we found significantly higher levels of TNF-$\alpha$ in the susceptible strains than in the resistant strains. The production of certain cytokines, i.e., CCL2, TNF-$\alpha$, and CXCL2, was significantly correlated with the MLD$_{50}$ ($P < 0.01$; $R^2 = 0.77$, 0.96, and 0.72, respectively). These results were similar to those identified earlier by array analysis.

**Viral load determines the outcome after infection with the HK213 virus.** We hypothesized that increased pathogenicity coupled with enhanced inflammation in the susceptible strains may be the result of higher viral titers. To test this hypothesis, we quantified the amount of infectious virus at days 2, 4, and 7 postinoculation with $10^4$ EID$_{50}$ of HK213 in the lungs of the 6 mouse
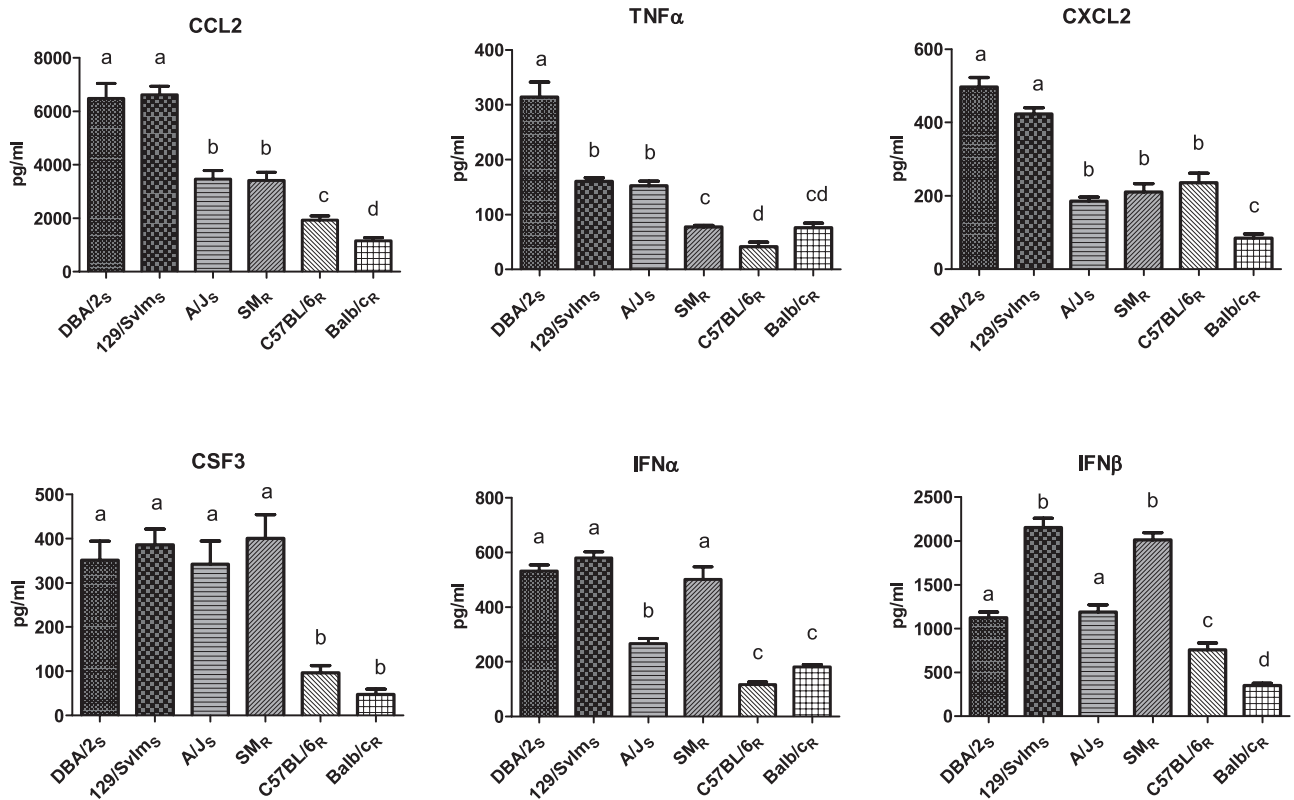
FIG 4 Elevated production of proinflammatory mediators in susceptible mouse strains after inoculation with H5N1 virus. Cytokine concentrations (pg/ml) were measured in homogenized lung tissues of DBA/2$_S$, 129/SvIm$_S$, A/J$_S$, SM$_R$, C57BL/6$_R$, and BALB/c$_R$ mice 3 days after inoculation with highly pathogenic A/Hong Kong/213/03 H5N1 virus. Bars represent mean cytokine production levels + SEMs. Statistical significance ($P < 0.01$) between the six mouse strains is represented by letters above each column, with different letters signifying distinct statistical groups.

strains used for expression and cytokine analysis. At day 2, the virus titer ranged from $10^{4.9}$ 50% tissue culture infective doses (TCID$_{50}$)/ml in C57BL/6$_R$ and SM$_R$ strains to $10^{6.5}$ TCID$_{50}$/ml in the DBA/2$_S$ strain (Table 1). The virus titer differed significantly between susceptible and resistant strains ($P < 0.05$), and it correlated well with the MLD$_{50}$ ($R^2 = 0.70$, $P < 0.05$). In addition, we found significant associations between virus titer and MLD$_{50}$ on day 4 ($R^2 = 0.82$, $P < 0.05$) and day 7 ($R^2 = 0.81$, $P < 0.05$). To estimate the viral burden over a period of 7 days, we calculated the area under the curve (AUC) for all 6 strains; again, we found a significant correlation with MLD$_{50}$ ($R^2 = 0.87$, $P < 0.01$).

To confirm the association between high viral load and in-

TABLE 1 Virus titers in the lungs of genetically diverse mouse strains inoculated with A/Hong Kong/213/03 H5N1 virus

| Mouse strain | Virus titer[a] ($\log_{10}$ TCID$_{50}$/ml) | | | |
|---|---|---|---|---|
| | Day 2 | Day 4 | Day 7 | Viral burden[b] (AUC) |
| DBA/2$_S$ | 6.5 | 5.7 | 4.8 | 34.6 |
| 129/SvIm$_S$ | 5.9 | 5.1 | 4.6 | 31.4 |
| A/J$_S$ | 5.8 | 5.0 | 4.0 | 30.0 |
| SM$_R$ | 4.9 | 4.6 | 3.2 | 26.1 |
| C57BL/6$_R$ | 4.9 | 5.0 | 3.6 | 27.8 |
| BALB/c$_R$ | 5.6 | 4.6 | 2.2 | 25.9 |

[a] Lung virus titers (50% tissue culture infectious doses [TCID$_{50}$s]) at days 2, 4, and 7 after inoculation with $10^4$ EID$_{50}$ of A/Hong Kong/213/03 influenza virus are shown.
[b] Area under the curve (AUC) for influenza virus titers between days 0 and 7 after inoculation with $10^4$ EID$_{50}$ of A/Hong Kong/213/03 influenza virus are shown.

creased susceptibility, we applied computer-assisted immunohistochemical analysis of lung tissue from 3 susceptible strains (DBA/2$_S$, 129/SvIm$_S$, and A/J$_S$) and 2 resistant strains (C57BL/6$_R$ and BALB/c$_R$) to detect the frequency of influenza A virus nucleoprotein-positive (NP$^+$) nuclei in cross sections of an entire formalin-fixed lung. Despite the small number of mice used in this experiment, it was clear that the susceptible strains had more NP$^+$ nuclei than did the resistant strains on days 2, 4, and 7 postinfection (see Table S3 in the supplemental material).

To demonstrate the effect of increased viral load on proinflammatory cytokine production and survival, we inoculated DBA/2$_S$ and C57BL/6$_R$ mice with a 100-fold-higher dose ($10^6$ EID$_{50}$). As predicted, the production of CCL2 and TNF-$\alpha$ 3 dpi was significantly higher ($P < 0.01$) (see Fig. S4 in the supplemental material) in the mice inoculated with $10^6$ EID$_{50}$ than in the mice inoculated with $10^4$ EID$_{50}$. More importantly, the amounts of CCL2 and TNF-$\alpha$ produced in the lethally infected C57BL/6$_R$ mice were similar to those found in DBA/2$_S$ mice infected with a much lower, but for this strain similarly lethal, dose of $10^4$ EID$_{50}$.

**Elevated production of proinflammatory mediators correlates with increased viral load in susceptible mouse strains.** The newfound associations between viral loads, proinflammatory cytokine production, and outcome after infection were confirmed using quantitative real-time PCR on a select set of proinflammatory mediators in conjunction with influenza A virus matrix RNA species. Twenty-four hours postinoculation, the amount of influenza virus RNA was significantly higher (analysis of variance
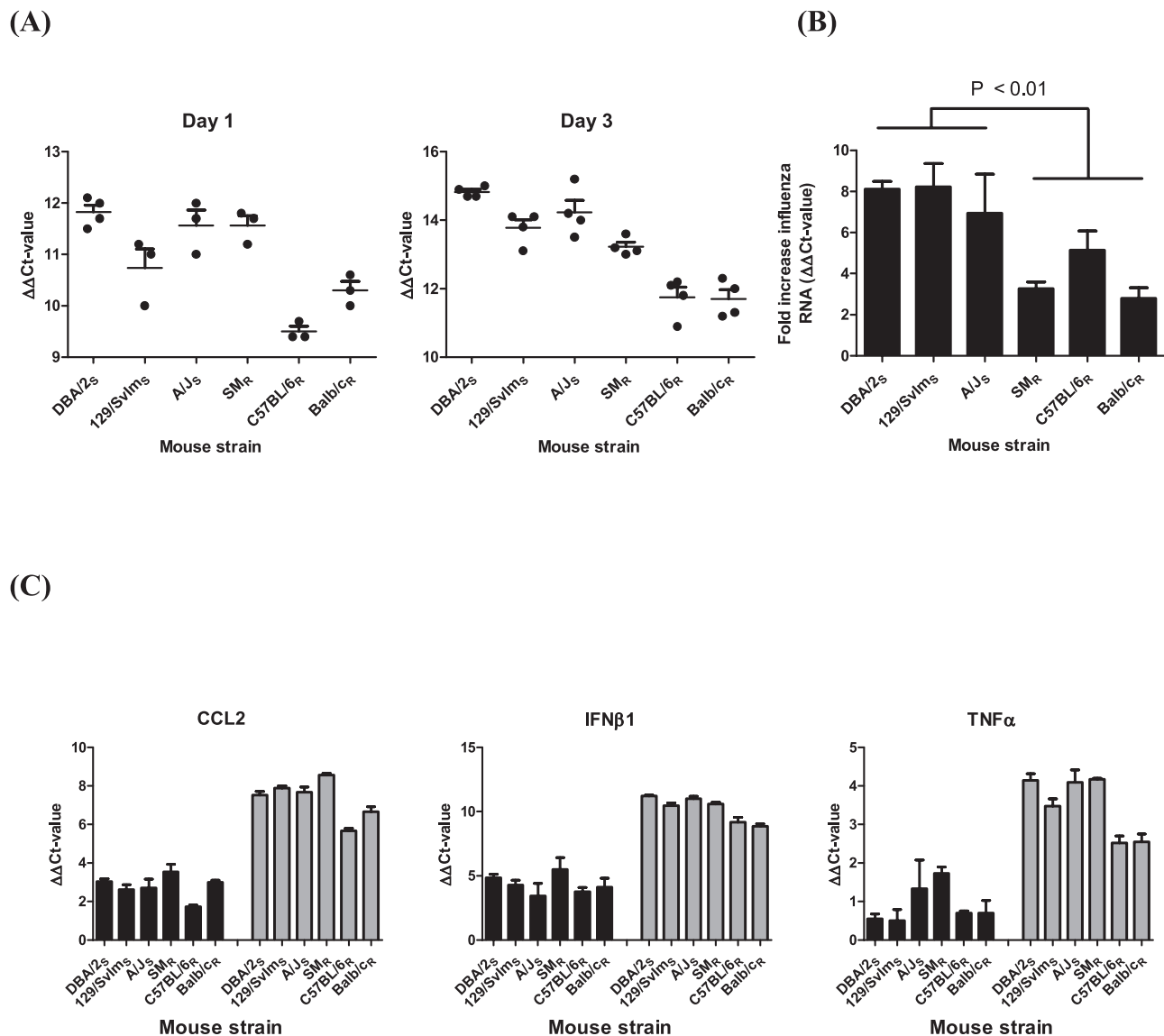
**(A)**

**(B)**



**(C)**



FIG 5 Viral load determines proinflammatory cytokine production in genetically diverse mice. (A) Higher viral load ($\Delta\Delta C_T$ value) in susceptible mouse strains (DBA/2$_S$, 129SvIm$_S$, and A/J$_S$) than in the resistant strains C57BL/6$_R$ and BALB/c$_R$ 1 and 3 days postinoculation (dpi) with $10^4$ EID$_{50}$ of H5N1 virus. Dots indicate individual mice, and the average values + SEMs are indicated by the solid bars. (B) Resistant mouse strains (SM$_R$, C57BL/6$_R$, and BALB/c$_R$) more effectively limit virus replication between 1 and 3 dpi than do susceptible strains. Bars represent average fold increases in viral RNA + SEMs. (C) Higher viral load in susceptible mouse strains plus SM$_R$ triggers an increase in production of proinflammatory mediators CCL2, IFN-$\beta$1, and TNF-$\alpha$ at 3 dpi (gray bars; $P < 0.01$) but not at 1 dpi (black bars; $P > 0.05$). Bars represent average $\Delta\Delta C_T$ values + SEMs.

[ANOVA], $P < 0.001$) in the three susceptible strains DBA/2$_S$, 129SvIm$_S$, and A/J$_S$ than in the two most resistant strains, C57BL/6$_R$ and BALB/c$_R$ (Fig. 5A). Not surprisingly the reduced viral load in the resistant strains minimized the production of proinflammatory cytokines on day 3 (Fig. 4) and allowed these two mouse strains to cluster at the transcriptional level (Fig. 3), displaying a "normal" inflammatory response to the invading pathogen. The third resistant strain, SM$_R$, had a high viral RNA load at 1 dpi similar to those of the susceptible strains and therefore clustered with a susceptible (A/J$_S$) strain at the transcriptional level and also produced more proinflammatory mediators. Three days postinoculation, the resistant C57BL/6$_R$ and BALB/c$_R$ strains continued to have smaller amounts of viral RNA (ANOVA,

$P < 0.0001$) than did the susceptible strains. In addition, the viral load in the third resistant strain, SM$_R$, was lower than those in all three susceptible strains, providing further support for our hypothesis that viral load dictates the pathogenic response to infection in genetically diverse mice. Interestingly, the increase in amount of viral RNA between 1 and 3 dpi is significantly lower ($P < 0.01$) in the resistant strains than in the susceptible strains (Fig. 5B), confirming that lower viral load and early control of viral replication are key to minimizing disease and promoting survival.

To exclude the possibility that excessive production of cytokines promotes virus replication and therefore increases the viral load, we determined the mRNA levels of several proinflammatory

mediators after inoculation with H5N1 influenza A virus. On day 1 postinoculation, the increases in expression of *ccl2*, *ifnb1*, and *tnfa* (threshold cycle [$\Delta\Delta C_T$] value) were similar between all 6 mouse strains (Fig. 5C; see also Fig. S3 in the supplemental material), indicating that the production of proinflammatory cytokines is not responsible for the observed difference in viral RNA at 3 dpi. At 3 dpi, the fold increase in mRNA associated with *ccl2*, *ifnb1*, and *tnfa* was significantly lower ($P < 0.001$) in the resistant strains C57BL/6$_R$ and BALB/c$_R$ than in the three susceptible strains plus SM/J$_R$, providing further support that early viral load determines the inflammatory response and as such the outcome after infection.

To demonstrate that the genetic differences do not affect the production of proinflammatory cytokines per unit of viral RNA, we computed the ratio between cytokine RNA and viral RNA $\Delta\Delta C_T$ values (see Fig. S3 in the supplemental material). At 1 and 3 dpi, the ratios for IFN-$\beta$1 were similar across all strains tested. For the other cytokines, we observed significant differences in the expression ratios among the different mouse strains; however, limited evidence for an association of these differences with disease severity or susceptibility to H5N1 virus infection was found. Combined, these analyses suggest not that the increased susceptibility is caused by an intrinsic difference in the response to infection but rather that it is caused by a higher viral load inducing excessive production of proinflammatory cytokines and hence increased morbidity and mortality in the susceptible mouse strains.

## DISCUSSION

Polymorphisms in the genome of the host play an important role in the severity of infection with a highly pathogenic H5N1 influenza A virus. The mechanism dictating the difference in H5N1 pathogenicities among genetically diverse hosts is, however, unknown. Detailed analysis of 6 H5N1 virus-infected inbred mouse strains demonstrated that the viral load is responsible for the heightened inflammation in susceptible hosts. This produces a pathogenic environment as early as 3 days postinoculation, ultimately causing the host to succumb.

Several studies have compared high- and low-pathogenic influenza A viruses in various host species and, without exception, identified a strong association between pathogenicity and excessive production of proinflammatory mediators (16, 18–25). Two possible mechanisms explain this difference: first, increased replication dynamics of the more pathogenic viruses may result in the infection of more epithelial cells and subsequent production of higher levels of cytokines. Second, altered intracellular signaling properties of viral proteins (e.g., PB1-F2, NS1, or hemagglutinin [HA]) of the pathogenic virus may trigger cells to produce more or different cytokines. Although both of these mechanisms are likely involved when comparing subtypes of influenza A viruses in a single homogenous host species, it is not well understood how a single highly pathogenic H5N1 virus produces such varied pathologies in genetically diverse hosts. Does the genetic change in susceptible hosts allow for increased replication dynamics or an altered immune environment, or does it completely change the hosts' response to the pathogen independently of viral burden?

Based on the data presented, we conclude that the susceptible host provides a milieu that allows for increased viral replication, which subsequently induces the production of more proinflammatory cytokines and tissue damage and ultimately results in the death of the animal. Although this study is the first of its kind,

detailed analysis of H5N1 virus-infected humans in Vietnam also demonstrated a significant correlation between viral load, cytokine concentration, and severity of disease (12), thereby supporting the conclusion that differences in pathogenesis within a single host species are the result of variable replication dynamics.

The difference in viral load between susceptible and resistant strains was presented very early after inoculation (24 to 48 h), suggesting that the virus replication rate in the susceptible mouse strains is higher than that in the resistant strains. At this point, it is unclear whether this increase in replication rate is due to an inefficient antiviral mechanism or to an increase in cell metabolism and/or the availability of nutrients required for replication. The observation that the viral load increased nearly 8-fold in the susceptible strains between 1 and 3 dpi compared to <4-fold in the resistant strains suggests that the increased replication rate is caused by one or more defective antiviral effector molecules induced by the production of type I and II interferons shortly after infection. Alternatively, there could be a difference in infectious dose (50% infectious dose [ID$_{50}$]) between the resistant and susceptible mouse strains due to variations such as the sialic acid receptor content of the respiratory tract. Previously, we had shown a 100% infection rate in a resistant strain and a susceptible strain following inoculation with a very low dose of 100 EID$_{50}$ of HK213, suggesting that the ID$_{50}$s are similar between resistant and susceptible mice and that this is unlikely the reason for the differences observed.

The importance of replication kinetics or polymerase activity in pathogenicity is well established (18, 26–30). The PB2$_{E627K}$ and PB2$_{D701N}$ mutations are associated with increased polymerase activity and faster replication; thus, viruses containing these mutations are often more pathogenic in mice (18, 27, 31). Molecular characterization of a variant PR8 virus adapted to induce severe disease in Mx1-positive mice found several mutations in the polymerase complex that allowed the virus to grow faster and therefore be more pathogenic than its wild-type counterpart (32). A recent comparison of A/Hong Kong/483/97 and A/Hong Kong/486/97 H5N1 viruses also surmised that replication rate regulates disease severity and the magnitude of the virus-specific CD8$^+$ T-cell response (18). After low-dose infection, the HK483 virus harboring a PB2 protein with a lysine residue at position 627 grew to significantly higher titers early during infection than did the variant containing a glutamic acid at this position. This difference in viral loads resulted in quantitative and qualitative differences in the cytotoxic T-cell responses that could be reversed upon administration of oseltamivir, a drug that limits viral replication. Combined, these studies suggest that the replication rate of the virus and hence viral load are responsible for the increase in inflammation and therefore pathogenesis of the virus. Reducing viral load or replication rate will most likely reduce morbidity and mortality upon infection.

As a result of the heightened viral load during the early stages of infection, the immune response in susceptible mice is excessive and can be detected within 3 days of infection. This relatively brief period of time has implications for potential intervention strategies for severe cases of influenza virus infection. It also explains the relatively short time period during which current commercially available antiviral therapy has proven effective. Similar observations have been made with monoclonal antibodies, whose treatment window is 3 to 4 days postinfection (33, 34). The opportunity to treat susceptible mice is much shorter (less than 1 day

postinfection) than that for resistant strains of mice (3 days postinfection [unpublished data]). In our study, one mouse strain that displayed an intermediate pathogenic profile ($SM_R$) recovered from the infection. This finding indicates that with the right treatment a pathogenic profile can be reversed and the animal can survive.

Clues about what biological trait is important for survival of influenza virus infection may be found in the $A/J_S$ and $SM_R$ strains. Although the strains had similar pathogenic expression profiles, the $SM_R$ mice survived the infection while the $A/J_S$ mice did not. The absence of glutathione metabolism pathway-associated gene expression in the $SM_R$ mice may provide us with a mechanism for the difference in pathogenesis. Glutathione metabolism gene transcription is initiated early after infection to reduce harmful reactive oxygen species (ROS). Mice lacking a functional NADPH oxidase (Cybb-deficient mice) can no longer produce ROS, and intranasal infection with influenza virus was shown to increase the production of proinflammatory cytokines and promote cellular infiltration into the lungs (35, 36). Despite the increase in inflammation, Cybb-deficient mice had lower viral loads and improved resolution of the infection, similar to what we observed in $SM_R$ mice. As such, further studies to determine the production of ROS and proinflammatory cytokines and to measure the induction of the glutathione metabolism response pathway in activated macrophages of $SM_R$ and $C57BL/6_R$ mice would be of interest. A lack of ROS production, minimal expression of glutathione response genes, and reduced proinflammatory cytokine production in the SM mouse macrophages will form the basis for future studies into the role of ROS in influenza virus pathogenesis. An alternative explanation is the presence of one or more genetic changes affecting viral clearance. An example of this is the hemolytic complement (Hc) gene, which affects T-cell responses and therefore viral load at later time points during infection. The $SM_R$ strain expresses a fully functional Hc gene; thus, viral load is reduced, inflammation is limited, and the animals are more likely to survive infection than are $A/J_S$ mice, which do not express a fully functional Hc gene.

Although the susceptible strains and $SM_R$ produced large amounts of proinflammatory cytokines (e.g., IFN-$\beta$ and CSF3), certain cytokines were predominantly produced in the extremely susceptible strains such as $DBA/2_S$ and $129/SvIm_S$. The excessive production of certain proinflammatory mediators such as CSF3 and type I interferons may cause a mild, controllable form of inflammation, though the addition of a second signal such as CCL2 and/or TNF-$\alpha$ may create an uncontrollable cascade of events resulting in tissue damage and diminished adaptive immune responses in these mice. Results from *in vitro* experiments suggest that IFN-$\beta$ and TNF-$\alpha$ act synergistically to induce a response quantitatively and qualitatively different from that of either cytokine alone (37, 38). Also, TNF-$\alpha$ affects morbidity after H5N1 virus infection (17, 39).

While the current study focused on identifying the mechanism of severe disease, e.g., virus replication, there is obvious merit in identifying the specific genetic polymorphisms responsible for this phenotype. The $MLD_{50}$ curve for highly pathogenic H5N1 virus (Fig. 1) suggests that several genetic polymorphisms are involved. A similar complexity was previously identified with the recombinant inbred BXD strain family, in which 3 genetic loci contribute to the response to influenza virus infection (40). To identify the responsible polymorphisms, genetic tools like the

BXD RI strains, consomic strain sets, or the Collaborative Cross will be extremely useful (41–44). Several of the candidate genes identified in our earlier BXD study were evaluated for their association with disease severity in our larger mouse panel using the available single nucleotide polymorphism (SNP) data. Hemolytic complement, on *Qivr2*, did not differentiate the resistant and susceptible mouse strains. *Qivr7* contains several potential antiviral genes (Trim genes); however, there are not enough public SNP data available to do the analysis. The candidate genes on *Qivr11* (*Grn*, *Ifi35*, and *Dhx58*) all associated significantly ($P < 0.01$) with disease severity and are currently under investigation for their role in influenza virus pathogenesis. Finally, none of the candidate genes on *Qivr17* (*Xdh*, *Eif2ak2*, *Emilin2*, and *Nlrc4*) separated with our phenotype.

In conclusion, gene polymorphisms in the genome of the infected host can have a profound impact on the course of an H5N1 influenza virus infection. Although featured as too much inflammation with excessive production of proinflammatory cytokines, the pathogenicity of influenza virus infection is rooted in increased virus titers in the lungs of the susceptible hosts.

## MATERIALS AND METHODS

**Inbred mouse strains and influenza A virus.** Female mice (6 to 8 weeks old) from the following strains were purchased from Jackson Laboratories (Bar Harbor, ME) and housed in the Animal Resource Center at St. Jude Children's Research Hospital: C57BL/6J (stock no. 664), BALB/cJ (stock no. 651), SM/J (stock no. 687), DBA/2J (stock no. 671), FVB/NJ (stock no. 1800), LP/J (stock no. 676), NZB/BlnJ (stock no. 684), C3H/HeJ (stock no. 659), BALB/cByJ (stock no. 1026), AKR/J (stock no. 648), B10.D2-H2/oSnJ (stock no. 461), A/J (stock no. 646), A/HeJ (stock no. 645), 129/SvImJ (stock no. 2448), MRL/MpJ (stock no. 486), NZW/LacJ (stock no. 1058), BTBR T+ tf/J (stock no. 2282), KK/HlJ (stock no. 2106), 129X1/SvJ (stock no. 691), DBA/1J (stock no. 670), and NOD/ShiLtJ (stock no. 1976). Strain selection was based on representation in large mouse genetic databases like Haplotype Mapping by Roche Pharmaceuticals, Ancestry Mapping by Perlegen, and full-genome sequencing by the Sanger Institute (45–47). The mice received water and food *ad libitum*, and all experimental procedures were approved by the Animal Care and Use Committee of St. Jude Children's Research Hospital.

A reverse genetics variant of A/Hong Kong/213/03, a highly pathogenic H5N1 influenza A virus, was propagated in 10-day-old embryonated chicken eggs. The allantoic fluid containing the infectious virus was harvested, and the infectious virus titer was determined in eggs. The A/Hong Kong/213/03 virus (H5N1) variant contains 7 segments of A/Hong Kong/213/03 and 1 segment of A/Chicken/Hong Kong/52/03 H5N1 virus (40). This virus is referred to as HK213 throughout the paper.

**Influenza A virus infection of mice.** Experimental inoculation of mice with HK213 virus was done intranasally in 30 $\mu$l phosphate-buffered saline (PBS) as described previously (40, 48). $MLD_{50}$ experiments were repeated, and the reported results were calculated from the cumulative results.

**Generation of bone marrow chimera DBA/2 mice.** $CD4^+$ and $CD8^+$ cells were depleted *in vivo* after intraperitoneal (i.p.) injection of $DBA/2_S$, $C57BL/6_R$, and $BALB/c_R$ donor mice with anti-CD4 and anti-CD8 antibodies. BM was then collected from the femurs of these mice, and approximately 6 million cells were injected intravenously into 9-Gy-irradiated $DBA/2_S$ mice. The mice were treated with Sulfatrim for 3.5 weeks to prevent any opportunistic infection.

At 12 weeks postengraftment, a small volume of peripheral blood was collected and subjected to flow cytometric analysis to test for the expression of cell surface markers of the respective donor mouse strains. In the $C57BL/6_R$ BM-recipient mice, we measured the percentage of $H-2^{b+}$ (C57BL/6) and $H-2^{k+}$ (DBA/2) cells within the $CD3^+$ T-cell population. In the $BALB/c_R$ BM-recipient mice, we measured the percentage of

CD22.1$^+$ (DBA/2) and CD22.2$^+$ (BALB/c) cells within the CD19$^+$ T-cell population. Animals in which more than 90% of the T or B cells were donor-derived cells were considered successful BM chimeras.

**Lung viral titers and immunohistochemistry.** Following intranasal inoculation with $10^4$ EID$_{50}$ of HK213 virus, lungs were harvested on days 2, 4, and 7 postinfection, and virus titers were determined on Madin-Darby canine kidney cells (40). At each time point, 4 to 6 animals from each mouse strain were used. The average virus titer was calculated, and the AUC was calculated between days 0 and 7 postinfection.

Immunohistochemical analysis was performed on formalin-fixed lung tissue harvested from HK213 virus-infected or uninfected DBA/2$_S$, 129/SvIm$_S$, A/J$_S$, C57BL/6$_R$, and BALB/c$_R$ mice, as described previously (40). Digital images were obtained with a ScanScope (Aperio, Vista, CA), and the percentage of NP-positive nuclei was determined with ImageScope (Aperio, Vista, CA) using a nucleus-based algorithm.

**Cytokine analysis.** Lungs from 6 strains of mice inoculated with $10^4$ EID$_{50}$ of HK213 virus were harvested on day 3 postinfection and homogenized in 1.0 ml PBS for two 30-s intervals at 30 Hz (TissueLyser II; Qiagen, Valencia, CA). After centrifugation for 30 s at 16,000 $\times$ $g$, the supernatant was collected, divided into aliquots, and stored at $-80°$C. The homogenates were subsequently thawed to quantify the amounts of CCL2, TNF-$\alpha$, CSF3, and CXCL2 in the lungs of infected animals by using Quantikine enzyme-linked immunosorbent assay (ELISA) kits (R&D Systems, Minneapolis, MN). The amounts of IFN-$\alpha$ and -$\beta$ in the lung were determined with the respective ELISA kits (PBL Laboratories, Piscataway, NJ). For each cytokine at a given time point, 4 to 6 animals were tested, and the average concentration $\pm$ standard error of the mean (SEM) is reported.

**RNA isolation and functional genomics.** Six mouse strains, DBA/2$_S$, 129SvIm$_S$, A/J$_S$, SM$_R$, C57BL/6$_R$, and BALB/c$_R$, were selected for an extensive RNA expression analysis before and after inoculation with $10^4$ EID$_{50}$ of HK213 virus. Lungs were isolated in 2 batches from uninfected mice and infected mice at days 1, 3, and 7 postinfection. RNA was extracted using TRIzol (Invitrogen, Carlsbad, CA), as previously reported (40) and submitted to a DNA cleanup protocol (Qiagen). Next, microarray analysis was done on RNA obtained from DBA/2$_S$, 129SvIm$_S$, A/J$_S$, SM$_R$, C57BL/6$_R$, and BALB/c$_R$ mice, using Illumina MouseWG-6 v1.1 Expression BeadChips (Illumina, San Diego, CA). PCA analysis identified a large batch effect; however, both batches included uninfected samples, which allowed us to calculate fold differences in gene expression. Also, batches were done according to the day postinfection, and all 6 strains were assessed simultaneously for each day.

Before analysis, probes without a signal (i.e., detection $P$ value of >0.05) in any of the 104 samples were removed from the data set. Signal values were ln-start transformed, ln(signal + 20), to stabilize variance across the range of intensities and approximate normalities in preparation for parametric tests. Using Partek Genomics Suite 6.3, we visualized the structure of the data via PCA. As a result of the complexity of the disease, we compared expression patterns of genes up- or downregulated in most of the susceptible or resistant strains. For a gene to qualify for an individual strain, we required a 2-fold increase or decrease in expression in the majority of the individual samples for that strain on that day. Once a gene qualified for a particular strain, we next assessed whether that gene was shared among the majority of the resistant or susceptible (2/3 or 3/4) mouse strains. Pathway analysis was performed using the online bioinformatics tool DAVID (49).

**Quantitative real-time PCR.** Samples of cDNA were prepared from lung tissue RNA (200 ng) by using Superscript III (Invitrogen) and random hexamers and used for quantitative real-time PCR. The $C_T$ values for murine interleukin-6 (IL-6) (Mm00446190_m1), CCL2 (Mm00441242_m1), CCL4 (Mm00443111_m1), IFN-$\beta$1 (Mm00439552_s1), TNF-$\alpha$ (Mm99999068_m1), CSF3 (Mm00438334_m1), and $\beta$-actin were determined using commercially available primer-probe pairs from Applied Biosystems (Foster City, CA). To quantify the amount of virus in each RNA sample, we used the cDNA prepared with random hexamers in combination

with a primer probe mix that was specific for the matrix gene (50). Baseline levels of each cytokine ($\Delta C_T$ value) were determined after normalization against $\beta$-actin, and the increase in expression ($\Delta\Delta C_T$ value) was calculated. No RNA species for IFN-$\beta$1, CSF3, or influenza virus matrix RNA were detected prior to infection. To calculate the increase, we used a $C_T$ value of 40 for the uninfected samples. RNA samples ($n = 3$ to 4) were tested for each strain and time point prior to or after infection with HK213 virus.

**Statistical analysis.** Statistical analysis of differences in lung virus titers was determined by a Student $t$ test following ln transformation of the data. Cytokine and chemokine production and quantitative PCR results were analyzed using a Student $t$ test or ANOVA when comparing more than two groups. For Fig. 4, statistical significance between the six mouse strains is represented by letters above each column, with different letters signifying distinct statistical groups. Linear regression analyses were done to analyze the viral load (log$_{10}$ TCID$_{50}$/ml and $\Delta\Delta C_T$ value) with MLD$_{50}$ (log$_{10}$ EID$_{50}$). $P$ values less than 0.05 were considered significant.

## SUPPLEMENTAL MATERIAL

Supplemental material for this article may be found at http://mbio.asm.org/lookup/suppl/doi:10.1128/mBio.00171-11/-/DCSupplemental.

Figure S1, PDF file, 0.1 MB.
Figure S2, PDF file, 0.1 MB.
Figure S3, PDF file, 0.1 MB.
Figure S4, PDF file, 0.1 MB.
Table S1, PDF file, 0.2 MB.
Table S2, PDF file, 0.1 MB.
Table S3, DOC file, 0.1 MB.

## REFERENCES

1. **Casrouge A, et al.** 2006. Herpes simplex virus encephalitis in human UNC-93B deficiency. Science **314**:308–312.
2. **Pereyra F, et al.** 2010. The major genetic determinants of HIV-1 control affect HLA class I peptide presentation. Science **330**:1551–1557.
3. **Pérez de Diego R, et al.** 2010. Human TRAF3 adaptor molecule deficiency leads to impaired Toll-like receptor 3 response and susceptibility to herpes simplex encephalitis. Immunity **33**:400–411.
4. **Rauch A, et al.** 2010. Genetic variation in IL28B is associated with chronic hepatitis C and treatment failure: a genome-wide association study. Gastroenterology **138**:1338–1345.
5. **Thomas DL, et al.** 2009. Genetic variation in IL28B and spontaneous clearance of hepatitis C virus. Nature **461**:798–801.
6. **Zhang SY, et al.** 2007. TLR3 deficiency in patients with herpes simplex encephalitis. Science **317**:1522–1527.
7. **Horby P, et al.** 2010. What is the evidence of a role for host genetics in susceptibility to influenza A/H5N1? Epidemiol. Infect. **138**:1550–1558.
8. **Olsen SJ, et al.** 2005. Family clustering of avian influenza A (H5N1). Emerg. Infect. Dis. **11**:1799–1801.
9. **Flint SM, et al.** 2010. Disproportionate impact of pandemic (H1N1) 2009 influenza on indigenous people in the top end of Australia's northern territory. Med. J. Aust. **192**:617–622.
10. **La Ruche G, et al.** 2009. The 2009 pandemic H1N1 influenza and indigenous populations of the Americas and the Pacific. Euro Surveill. **14**: 19366.
11. **Chan RW, et al.** 2010. Influenza H5N1 and H1N1 virus replication and innate immune responses in bronchial epithelial cells are influenced by the state of differentiation. PLoS One **5**:e8713.
12. **de Jong MD, et al.** 2006. Fatal outcome of human influenza A (H5N1) is

associated with high viral load and hypercytokinemia. Nat. Med. 12:1203–1207.

13. Hui KP, et al. 2009. Induction of proinflammatory cytokines in primary human macrophages by influenza A virus (H5N1) is selectively regulated by IFN regulatory factor 3 and p38 MAPK. J. Immunol. 182:1088–1098.

14. Mok KP, et al. 2009. Viral genetic determinants of H5N1 influenza viruses that contribute to cytokine dysregulation. J. Infect. Dis. 200:1104–1112.

15. Peiris JS, et al. 2004. Re-emergence of fatal human influenza A subtype H5N1 disease. Lancet 363:617–619.

16. Perrone LA, Plowden JK, Garcia-Sastre A, Katz JM, Tumpey TM. 2008. H5N1 and 1918 pandemic influenza virus infection results in early and excessive infiltration of macrophages and neutrophils in the lungs of mice. PLoS Pathog. 4:e1000115.

17. Szretter KJ, et al. 2007. Role of host cytokine responses in the pathogenesis of avian H5N1 influenza viruses in mice. J. Virol. 81:2736–2744.

18. Hatta Y, et al. 2010. Viral replication rate regulates clinical outcome and CD8 T cell responses during highly pathogenic H5N1 influenza virus infection in mice. PLoS Pathog. 6:e1001139.

19. Baskin CR, et al. 2009. Early and sustained innate immune response defines pathology and death in nonhuman primates infected by highly pathogenic influenza virus. Proc. Natl. Acad. Sci. U. S. A. 106:3455–3460.

20. Cilloniz C, et al. 2010. Lethal dissemination of H5N1 influenza virus is associated with dysregulation of inflammation and lipoxin signaling in a mouse model of infection. J. Virol. 84:7613–7624.

21. Cilloniz C, et al. 2009. Lethal influenza virus infection in macaques is associated with early dysregulation of inflammatory related genes. PLoS Pathog. 5:e1000604.

22. Fornek JL, et al. 2009. A single-amino-acid substitution in a polymerase protein of an H5N1 influenza virus is associated with systemic infection and impaired T-cell activation in mice. J. Virol. 83:11102–11115.

23. Kobasa D, et al. 2007. Aberrant innate immune response in lethal infection of macaques with the 1918 influenza virus. Nature 445:319–323.

24. Kobasa D, et al. 2004. Enhanced virulence of influenza A viruses with the haemagglutinin of the 1918 pandemic virus. Nature 431:703–707.

25. Lee SM, et al. 2008. Hyperinduction of cyclooxygenase-2-mediated proinflammatory cascade: a mechanism for the pathogenesis of avian influenza H5N1 infection. J. Infect. Dis. 198:525–535.

26. Chen LM, Davis CT, Zhou H, Cox NJ, Donis RO. 2008. Genetic compatibility and virulence of reassortants derived from contemporary avian H5N1 and human H3N2 influenza A viruses. PLoS Pathog. 4:e1000072.

27. Hatta M, Gao P, Halfmann P, Kawaoka Y. 2001. Molecular basis for high virulence of Hong Kong H5N1 influenza A viruses. Science 293:1840–1842.

28. Hulse-Post DJ, et al. 2007. Molecular changes in the polymerase genes (PA and PB1) associated with high pathogenicity of H5N1 influenza virus in mallard ducks. J. Virol. 81:8515–8524.

29. Leung BW, Chen H, Brownlee GG. 2010. Correlation between polymerase activity and pathogenicity in two duck H5N1 influenza viruses suggests that the polymerase contributes to pathogenicity. Virology 401:96–106.

30. Salomon R, et al. 2006. The polymerase complex genes contribute to the high virulence of the human H5N1 influenza virus isolate A/Vietnam/1203/04. J. Exp. Med. 203:689–697.

31. Li Z, et al. 2005. Molecular basis of replication of duck H5N1 influenza viruses in a mammalian mouse model. J. Virol. 79:12058–12064.

32. Grimm D, et al. 2007. Replication fitness determines high virulence of influenza A virus in mice carrying functional Mx1 resistance gene. Proc. Natl. Acad. Sci. U. S. A. 104:6806–6811.

33. Hanson BJ, et al. 2006. Passive immunoprophylaxis and therapy with humanized monoclonal antibody specific for influenza A H5 hemagglutinin in mice. Respir. Res. 7:126.

34. Simmons CP, et al. 2007. Prophylactic and therapeutic efficacy of human monoclonal antibodies against H5N1 influenza. PLoS Med. 4:e178.

35. Snelgrove RJ, Edwards L, Rae AJ, Hussell T. 2006. An absence of reactive oxygen species improves the resolution of lung influenza infection. Eur. J. Immunol. 36:1364–1373.

36. Vlahos R, et al. 2011. Inhibition of Nox2 oxidase activity ameliorates influenza A virus-induced lung inflammation. PLoS Pathog. 7:e1001271.

37. Bartee E, McFadden G. 2009. Human cancer cells have specifically lost the ability to induce the synergistic state caused by tumor necrosis factor plus interferon-beta. Cytokine 47:199–205.

38. Bartee E, Mohamed MR, Lopez MC, Baker HV, McFadden G. 2009. The addition of tumor necrosis factor plus beta interferon induces a novel synergistic antiviral state against poxviruses in primary human fibroblasts. J. Virol. 83:498–511.

39. Belisle SE, et al. 2010. Genomic profiling of tumor necrosis factor alpha (TNF-alpha) receptor and interleukin-1 receptor knockout mice reveals a link between TNF-alpha signaling and increased severity of 1918 pandemic influenza virus infection. J. Virol. 84:12576–12588.

40. Boon AC, et al. 2009. Host genetic variation affects resistance to infection with a highly pathogenic H5N1 influenza A virus in mice. J. Virol. 83:10417–10426.

41. Aylor DL, et al. 2011. Genetic analysis of complex traits in the emerging Collaborative Cross. Genome Res. 21:1213–1222.

42. Chesler EJ, et al. 2005. Complex trait analysis of gene expression uncovers polygenic and pleiotropic networks that modulate nervous system function. Nat. Genet. 37:233–242.

43. Iraqi FA, Churchill G, Mott R. 2008. The Collaborative Cross, developing a resource for mammalian systems genetics: a status report of the Wellcome Trust cohort. Mamm. Genome 19:379–381.

44. Xiao J, et al. 2010. A novel strategy for genetic dissection of complex traits: the population of specific chromosome substitution strains from laboratory and wild mice. Mamm. Genome 21:370–376.

45. Frazer KA, et al. 2007. A sequence-based variation map of 8.27 million SNPs in inbred mouse strains. Nature 448:1050–1053.

46. Liao G, et al. 2004. In silico genetics: identification of a functional element regulating H2-Ealpha gene expression. Science 306:690–695.

47. Zheng M, Shafer S, Liao G, Liu HH, Peltz G. 2009. Computational genetic mapping in mice: the ship has sailed. Sci. Transl. Med. 1:3ps4.

48. Boon AC, et al. 2010. Cross-reactive neutralizing antibodies directed against pandemic H1N1 2009 virus are protective in a highly sensitive DBA/2 mouse influenza model. J. Virol. 84:7662–7667.

49. Huang DW, Sherman BT, Lempicki RA. 2009. Systematic and integrative analysis of large gene lists using DAVID bioinformatics resources. Nat. Protoc. 4:44–57.

50. Di Trani L, et al. 2006. A sensitive one-step real-time PCR for detection of avian influenza viruses using a MGB probe and an internal positive control. BMC Infect. Dis. 6:87.